Anisotropic magnetodielectric effect in the honeycomb-type magnet α-$RuCl_3$

Takuya Aoyama,[1] Yoshinao Hasegawa,[1] Shojiro Kimura,[2] Tsuyoshi Kimura,[3] and Kenya Ohgushi[1]

[1]*Department of Physics, Graduate School of Science, Tohoku University, 6-3, Aramaki Aza-Aoba, Aoba-ku, Sendai, Miyagi 980-8578, Japan*

[2]*Institute for Materials Research, Tohoku University, Sendai 980-8577, Japan*

[3]*Division of Material Physics, Graduate School of Engineering Science, Osaka University, Toyonaka, Osaka 560-8531, Japan*

(Received 16 February 2017; published 5 June 2017)

The magnetoelectric coupling in possible Kitaev spin liquid α-$RuCl_3$ with the layered honeycomb structure was examined. We observed a remarkable anisotropic magnetodielectric effect in the zigzag-type antiferromagnetic phase; there is a large suppression in dielectric constant, when both electric and magnetic fields were applied parallel to the in-plane direction. A possible origin of the observed anisotropic magnetodielectric effect is discussed in terms of a magnetically induced local electric polarization with antiferroelectric correlation. Our results stimulate the model calculation including not only exchange coupling but also magnetoelectric coupling to understand the ground state of the spin system in α-$RuCl_3$.

DOI: 10.1103/PhysRevB.95.245104

I. INTRODUCTION

The Kitaev model, which is the Ising model with bond-dependent anisotropic interactions on the honeycomb lattice, involves the magnetic frustration. The Kitaev model can be mathematically solved using two types of Majorana fermions, and it is exactly shown that the ground state is a Z_2 quantum spin liquid, so called Kitaev spin liquid, in which only the nearest-neighbor spin correlations become finite [1,2]. In addition, it was demonstrated that two kinds of Majorana fermions, which are itinerant and localized Majorana fermions, will appear in physical quantities such as specific heat, NMR relaxation rate, and so on; therefore, the experimental observation of Majorana fermions is possible [3]. The Kitaev spin liquid is possibly realized in the real materials since it is to some extent robust against perturbations, such as the conventional Heisenberg interaction [4]. The candidate materials are honeycomb iridates such as Na_2IrO_3, in which Ir^{4+} ions with $(5d)^5$ electron configurations show the so-called $J_{\mathrm{eff}} = 1/2$ electronic state due to the strong spin-orbit coupling in $5d$ transition metal ions [5,6]. It has been reported that Na_2IrO_3 actually has Kitaev-type interaction, which is about 10 times larger than the conventional Heisenberg-type interaction though it shows a magnetically ordered state at low temperature [7]. The other materials studied so far as the candidate for Kitaev spin liquid are Li_2IrO_3 [8] and its structural isomers [9,10], Li_2RhO_3 [11], and α-$RuCl_3$ [12].

α-$RuCl_3$ targeted in this work is a two-dimensional honeycomb lattice antiferromagnet with $(4d)^5$ electron configurations in the low-spin state (Fig. 1). Since the Ru^{3+} ions are subject to the trigonal crystal field, which is as large as the spin-orbit coupling, the material can be viewed as an XY spin system showing strong in-plane anisotropy [13]. Despite being the $4d$ electron system with smaller spin-orbit coupling in comparison with the $5d$ electron system, the excellence of Kitaev interaction as well as resultant Kitaev-like magnetism was demonstrated by many experimental results including two broad peaks of specific heat, an abnormal dispersion in the inelastic neutron spectra, and the Fermionic component in the Raman spectra [13–18]. However, the system undergoes an antiferromagnetic transition at low temperatures and the in-plane magnetic structure is a zigzag type. The magnetic transition temperature and the periodicity along the c^* axis vary depending on the type of polymorphs, $T_{N1} = 8$ K in ABC-type polymorph and $T_{N2} = 14$ K in AB-type polymorph, which emerge owing to small perturbations such as impurities and stress [19].

In various frustrated spin systems, the magnetically ordered state is stabilized by the coupling with lattice and/or charge degrees of freedom, which release the entropy of the spin system. The typical examples are the magnetoelectric (ME) effect in multiferroic $TbMnO_3$, the spin dimerization in organic Cu salts, and the spin-driven Jahn-Teller transition in spinel chromites [20–22]. It is expected that the coupling between the spin and the lattice will greatly influence its ground state, especially in the system with strong spin-orbit coupling. Measurements of the ME and the magnetodielectric (MD) effects are effective methods to detect the coupling between the spin and other degrees of freedom. Therefore, in this paper we evaluated the ME and MD coupling in α-$RuCl_3$.

II. EXPERIMENT

Single crystals of α-$RuCl_3$ were grown by the chemical vapor transport method using a two-zone furnace. Anhydrous $RuCl_3$ (Mitsuwa Chemicals Co. Ltd., purity 99.9%) was used as an initial reagent The obtained sample has ab surfaces in common with its own form and its typical dimension is $5\times5\times0.3\,\mathrm{mm}^3$. The samples were characterized by the magnetic susceptibility measurements, from which we conclude that our samples are mainly AB-type polymorph with $T_{N2} = 14$ K [23]. The crystals were cut into thin plates with the widest plane parallel or perpendicular to the c^* axis for dielectric constant measurements (the in-plane direction was not determined). The relative dielectric constant (ε') was measured by using an LCR meter (Agilent E4980A) in a magnetic field (B) generated by a commercial superconducting magnet. The measurement frequency (f) was set to 5–300 kHz.

III. RESULTS AND DISCUSSIONS

The temperature (T) profiles of ε' are shown in Fig. 2. A peculiar anisotropic MD response was observed. As shown in Fig. 2(c), no remarkable T variation in ε'_c was observed when an electric field (E) was applied along the c^* axis,

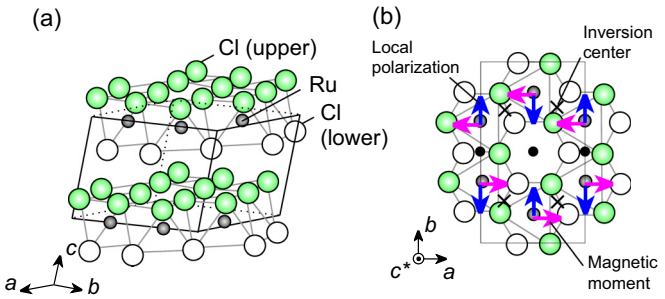

FIG. 1. (a) The crystal structure of α-$RuCl_3$. Ruthenium atom is shown in gray, chlorine on the upper (lower) side of the honeycomb layer is shown in pale green (white). Space group is $C2/m$. (b) The structure of single honeycomb layer. The solid squared line represents the unit cell. Black crosses and black filled circles indicate the inversion center. The inversion symmetry at black filled circles is broken by the zigzag-type magnetic order. Red arrows represent the magnetic moment of Ru^{3+} ions. Blue arrows indicate possible local electric polarizations.

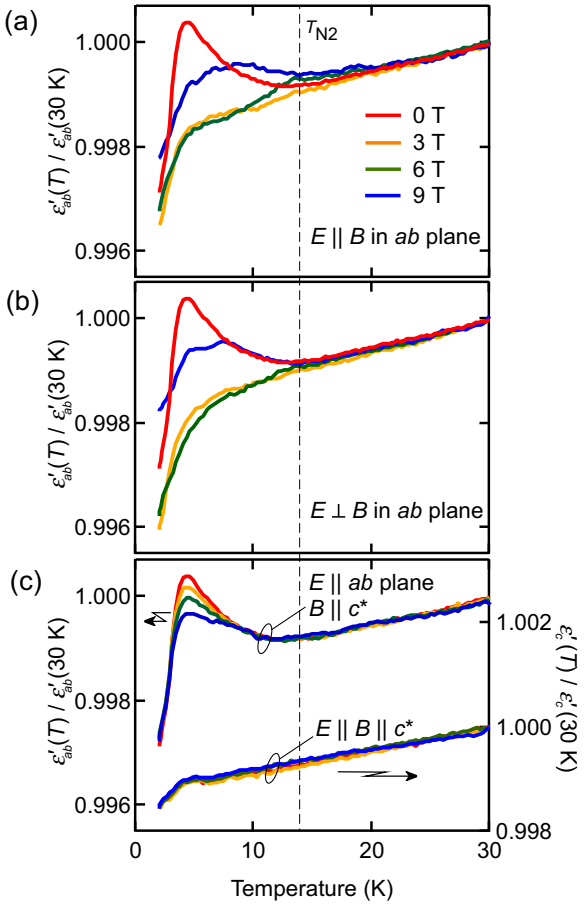

FIG. 2. The temperature dependence of the dielectric constant measured at $f = 100$ kHz by applying electric and magnetic fields in various directions with respect to the crystal axes. The configurations are (a) $E \parallel B$ in the ab plane, (b) $E \perp B$ in the ab plane, and (c) $E \parallel ab$, $B \parallel c^*$, and E, $B \parallel c^*$. In order to clearly show the change due to the magnetic field, the data scaled with the dielectric constant measured at 30 K in each applied magnetic field are shown. The dotted line indicates the Néel temperature of our specimen determined by magnetization measurements.

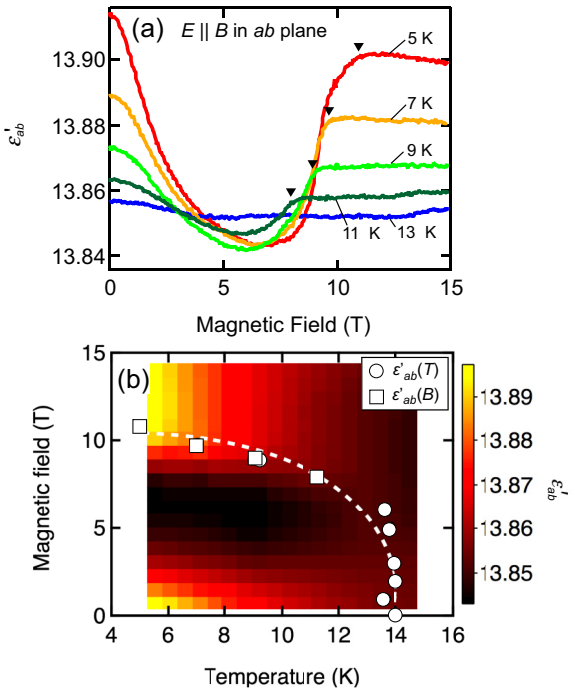

FIG. 3. (a) Isothermal magnetodielectric effect when electric and magnetic fields are applied in the ab plane with $E \parallel B$. (b) Temperature and magnetic field phase diagram with the contour plot of a dielectric constant collected at the $E \parallel B$ configuration. The circles (squares) in the phase diagram are determined by the temperature (magnetic field) dependence of ε'_{ab}.

and ε'_c shows negligible B dependence. On the other hand, in the case of applying E along the ab plane at $B = 0$ T, ε'_{ab} begins to increase following the Curie-Weiss law below around $T_{N2} = 14$ K [Figs. 2(a) and 2(b)]. The increased ε'_{ab} shows a broad peak at around 3 K and then decreases with further decreasing T.

The most noticeable result is that the anomaly appearing in ε'_{ab} shows the nonmonotonic and anisotropic B dependencies. As shown in Fig. 2(c), applying the B along the c^* axis has little influence on ε'_{ab}, while nonmonotonous change appears when B is applied in the ab plane [Figs. 2(a) and 2(b)]. The remarkable influence of B applied parallel to the ab plane is related to the fact that the in-plane magnetic susceptibility is larger than the c^*-axis one. By the application of B in the ab plane, ε'_{ab} first decreases and the peak structure observed at around 3 K at $B = 0$ T is suppressed gradually and disappears above 3 T; however, ε'_{ab} becomes larger again by further increasing B. The anisotropy between the longitudinal and transverse configurations shown in Figs. 2(a) and 2(b) is relatively small. Though the peak structure in ε'_{ab} and its B dependence are reminiscent of magnetically induced ferroelectricity observed in some multiferroics like $TbMnO_3$ [20], no significant macroscopic polarization was observed in any measured arrangements (data not shown)

Figure 3(a) shows the result of isothermal MD effect, on which we will show in detail the nonmonotonic change in ε'_{ab} against B applied parallel to the ab plane. In this configuration, a downwardly convex MD effect is clearly observed below 11 K. As indicated by black triangles in Fig. 3(a), the kink

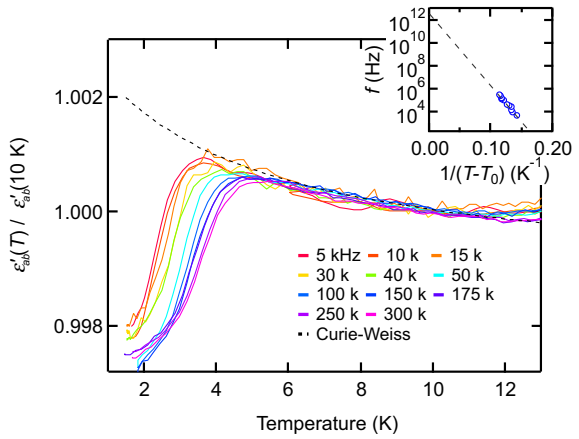

FIG. 4. (a) Temperature dependence of the dielectric constant in the absence of magnetic field measured at various frequencies (5–300 kHz). The black dotted line is fitting with Curie-Weiss law. The inset shows the derivation of relaxation energy by the Vogel-Fulcher law $f = f_0 \exp[-E/k_B(T - T_0)]$. Here k_B is the Boltzmann constant.

observed around 10 T at 5 K shifts toward the lower B side as T increases. This kink is considered to be the transition from the antiferromagnetic phase to the forced ferromagnetic phase. The T-B phase diagram of α-$RuCl_3$ based on the phase boundary determined by the data in Figs. 2(a) and 3(a) is shown in Fig. 3(b). The dielectric anomaly at $T_{N2} = 14$ K was suppressed to the low T side with the application of B and disappears at around 10 T. Since this behavior is consistent with the T-B phase diagram of the previous studies deduced from the magnetic susceptibility data [13,24], it is concluded that the MD effect observed in this study is indeed a characteristic of the magnetic ordered phase having the zigzag-type structure in an AB-type polymorph.

On the basis of the symmetry argument, it is expected that the MD effect in magnetic insulators is proportional to $\langle S^i_{\vec{q}} S^j_{-\vec{q}} \rangle$, which is the thermal average of the instantaneous spin-spin correlation at the magnetic wave vector $\vec{q}$ [25]. This means the MD effect observed in magnetic insulators is proportional to the square of sublattice magnetization. On the other hand, in α-$RuCl_3$, the remarkable increasing in the ε'_{ab} was observed on the low B side. This corresponds to the Curie-like divergence of ε'_{ab} due to the dielectric fluctuation which develops markedly below T_{N2}.

Next, in order to investigate the details of the peak structure appearing at around $T = 3$ K, we collected T dependence of ε'_{ab} data with several f (Fig. 4). At any measured f, the high T side of ε'_{ab} follows the simple Curie-Weiss law and its Weiss temperature is negative, indicating the antiferroic interaction. The peak structure observed at around 3 K shows strong f dependence. As seen in Fig. 4, the peak position monotonically shifts toward the lower T side, and the peak height increases with decreasing f. When plotting the measured f against the peak temperature of ε'_{ab}, we notice that the curve does not follow the simple Arrhenius law; instead, it can be well fitted by the Vogel-Fulcher law [26,27] with $T_0 = -4$ K (the inset of Fig. 4). The estimated activation energy E is 154 K, and the characteristic frequency f_0 is about 10^{12} Hz. These features resemble those of the ac magnetic susceptibility in canonical spin glasses [28] and the ac dielectric constant in relaxor ferroelectrics [29], suggesting that a glassy state contributes to the peak structure in ε'_{ab}. One interpretation deduced from the obtained results is that the local polarizations are induced upon the zigzag-type antiferromagnetic order at 14 K, form antiferroelectric correlation on cooling, and are finally frozen at around 3 K. This interpretation as the glass transition is in harmony with an indiscernible anomaly in the specific heat at around 3 K [13].

The appearance of the local polarization is well explained from the viewpoint based on the magnetic symmetry. According to the neutron diffraction measurements for the AB-polymorph α-$RuCl_3$, the antiferromagnetically ordered phase below 14 K has the zigzag-type structure, which is also realized in Na_2IrO_3 [14]. Let us first consider the magnetic symmetry for a single honeycomb layer. The honeycomb lattice in α-$RuCl_3$ has slightly deformed owing to the monoclinic distortion and has a point group of $2/m$ [Fig. 1(b)], which is lower than the point group of $\bar{3}m$ in an ideal honeycomb structure. When the zigzag-type structure with easy axis along the a axis is formed, the inversion center at the bond where the reversed spins are adjacent to each other is lost [shown as black filled circles in Fig. 1(b)]. Then, the local polarization emerges due to this local inversion symmetry breaking. Because of the remaining inversion centers, the local polarization will be arranged in an alternating manner, so that the total polarization in a single honeycomb layer becomes zero. The magnetic point group of α-$RuCl_3$ determined by the neutron diffraction experiments is actually $2/m$, in which an antiferroelectric order is certainly allowed [30]. We then expect the material exhibits the long-range antiferroelectric order below T_{N2}; however, our experiments indicate the glassy antiferroelectric transition far below T_{N2}. This discrepancy is well explained by the randomness in the stacking fault, which is actually observed as the diffusive $00l$ Bragg peak along the c^* direction in the x-ray diffraction measurements [24]. As a result, it is presumed that the long-range in-plane dielectric order cannot evolve sufficiently along the stacking direction, resulting in the glassy state at around 3 K. The separation of the magnetic and dielectric transition temperature is probably due to the dielectric property and is influenced more sensitively by the stacking fault than the magnetic property.

Finally, we briefly discuss a possible novel quantum state realized in a Kitaev magnet with strong ME coupling. It is theoretically predicted that the gap will open at the Dirac point of Majorana fermion bands upon irradiation of the circularly polarized laser, if there is the ME coupling in Kitaev magnets [31]. To observe the Dirac point related phenomena, it is necessary to cool the specimen to an extremely low temperature at which there is no gapped excitation of localized Majorana fermions. We can therefore conclude that searching for a new material that shows pure Kitaev characteristics even at low temperature is necessary.

IV. SUMMARY

To summarize, we examined the magnetoelectric properties in α-$RuCl_3$, which is the XY antiferromagnet with strong Kitaev interaction. The remarkable magnetodielectric effect was observed in the zigzag-type magnetic ordered state below

14 K, particularly when electric and magnetic fields were applied in the honeycomb layer. At around 3 K, the dielectric constant shows a broad peak, which exhibits strong frequency dependence. This feature is well understood as the relaxor antiferroelectrics, in which the local polarization is induced by the formation of the zigzag-type magnetic order. From the present results, we can conclude that it is indispensable to consider both spin and lattice degrees of freedom to fully understand the ground state of α-$RuCl_3$.

ACKNOWLEDGMENTS

We are grateful to T. Nojima for the support in the magnetic measurements. This work was partly performed at the High field Laboratory for Superconducting Materials, Institute for Materials Research, Tohoku University (Project No.16H0205). The present work is financially supported by JSPS KAKENHI No. 16K17732, No. 26287073, No. 20379316, and No. 16H01062.

[1] A. Kitaev, Ann. Phys. **321**, 2 (2006).
[2] G. Baskaran, S. Mandal, and R. Shankar, Phys. Rev. Lett. **98**, 247201 (2007).
[3] J. Nasu, M. Udagawa, and Y. Motome, Phys. Rev. B **92**, 115122 (2015).
[4] J. Chaloupka, G. Jackeli, and G. Khaliullin, Phys. Rev. Lett. **110**, 097204 (2013).
[5] G. Jackeli and G. Khaliullin, Phys. Rev. Lett. **102**, 017205 (2009).
[6] Y. Singh and P. Gegenwart, Phys. Rev. B **82**, 064412 (2010).
[7] Y. Yamaji, Y. Nomura, M. Kurita, R. Arita, and M. Imada, Phys. Rev. Lett. **113**, 107201 (2014).
[8] Y. Singh, S. Manni, J. Reuther, T. Berlijn, R. Thomale, W. Ku, S. Trebst, and P. Gegenwart, Phys. Rev. Lett. **108**, 127203 (2012).
[9] T. Takayama, A. Kato, R. Dinnebier, J. Nuss, H. Kono, L. Veiga, G. Fabbris, D. Haskel, and H. Takagi, Phys. Rev. Lett. **114**, 077202 (2015).
[10] K. A. Modic, T. E. Smidt, I. Kimchi, N. P. Breznay, A. Biffin, S. Choi, R. D. Johnson, R. Coldea, P. Watkins-Curry, G. T. McCandless, J. Y. Chan, F. Gandara, Z. Islam, A. Vishwanath, A. Shekhter, R. D. McDonald, and J. G. Analytis, Nat. Commun. **5**, 4203 (2014).
[11] P. Khuntia, S. Manni, F. R. Foronda, T. Lancaster, S. J. Blundell, P. Gegenwart, and M. Baenitz, arXiv:1512.04904.
[12] K. W. Plumb, J. P. Clancy, L. J. Sandilands, V. V. Shankar, Y. F. Hu, K. S. Burch, H.-Y. Kee, and Y.-J. Kim, Phys. Rev. B **90**, 041112 (2014).
[13] Y. Kubota, H. Tanaka, T. Ono, Y. Narumi, and K. Kindo, Phys. Rev. B **91**, 094422 (2015).
[14] A. Banerjee, C. A. Bridges, J.-Q. Yan, A. A. Aczel, L. Li, M. B. Stone, G. E. Granroth, M. D. Lumsden, Y. Yiu, J. Knolle, S. Bhattacharjee, D. L. Kovrizhin, R. Moessner, D. A. Tennant, D. G. Mandrus, and S. E. Nagler, Nat. Mater. **15**, 733 (2016).
[15] J. Nasu, J. Knolle, D. L. Kovrizhin, and Y. Motome, Nat. Phys. **12**, 912 (2016).
[16] L. J. Sandilands, Y. Tian, K. W. Plumb, Y.-J. Kim, and K. S. Burch, Phys. Rev. Lett. **114**, 147201 (2015).
[17] A. Banerjee, J. Yan, J. Knolle, C. A. Bridges, M. B. Stone, M. D. Lumsden, D. G. Mandrus, D. A. Tennant, R. Moessner, and S. E. Nagler, arXiv:1609.00103.
[18] K. Ran, J. Wang, W. Wang, Z.-Y. Dong, X. Ren, S. Bao, S. Li, Z. Ma, Y. Gan, Y. Zhang *et al.*, Phys. Rev. Lett. **118**, 107203 (2017).
[19] H. B. Cao, A. Banerjee, J. Q. Yan, C. A. Bridges, M. D. Lumsden, D. G. Mandrus, D. A. Tennant, B. C. Chakoumakos, and S. E. Nagler, Phys. Rev. B **93**, 134423 (2016).
[20] T. Kimura, T. Goto, H. Shintani, K. Ishizaka, T. Arima, and Y. Tokura, Nature (London) **426**, 55 (2003).
[21] M. Abdel-Jawad, I. Terasaki, T. Sasaki, N. Yoneyama, N. Kobayashi, Y. Uesu, and C. Hotta, Phys. Rev. B **82**, 125119 (2010).
[22] Y. Yamashita and K. Ueda, Phys. Rev. Lett. **85**, 4960 (2000).
[23] See Supplemental Material at http://link.aps.org/supplemental/10.1103/PhysRevB.95.245104 for the magnetization measurement.
[24] R. D. Johnson, S. C. Williams, A. A. Haghighirad, J. Singleton, V. Zapf, P. Manuel, I. I. Mazin, Y. Li, H. O. Jeschke, R. Valentí, and R. Coldea, Phys. Rev. B **92**, 235119 (2015).
[25] G. Lawes, A. P. Ramirez, C. M. Varma, and M. A. Subramanian, Phys. Rev. Lett. **91**, 257208 (2003).
[26] H. Vogel, Phys. Z. **22**, 645 (1921).
[27] G. S. Fulcher, J. Am. Ceram. Soc. **8**, 339 (1925).
[28] R. N. Bhowmik and R. Ranganathan, J. Magn. Magn. Mater. **248**, 101 (2002).
[29] A. A. Bokov and Z.-G. Ye, J. Mater. Sci. **41**, 31 (2006).
[30] A. P. Cracknell, *Magnetism in Crystalline Materials* (Pergamon Press, Oxford, 1975).
[31] M. Sato, Y. Sasaki, and T. Oka, arXiv:1404.2010.